AGU PUBLICATIONS

JGR

Journal of Geophysical Research: Atmospheres

RESEARCH ARTICLE
10.1002/2013JD020693

Key Points:
- The RegCM4's predictability of precipitation over East Asia is assessed
- Precipitation changes adapted to the RCP scenarios are projected
- Current and future precipitation patterns over East Asia are characterized

Correspondence to:
M.-S. Suh,
sms416@kongju.ac.kr

Citation:
Oh, S.-G., J.-H. Park, S.-H. Lee, and M.-S. Suh (2014), Assessment of the RegCM4 over East Asia and future precipitation change adapted to the RCP scenarios, *J. Geophys. Res. Atmos.*, *119*, 2913–2927, doi:10.1002/2013JD020693.

Received 8 AUG 2013
Accepted 24 JAN 2014
Accepted article online 13 MAR 2014
Published online 20 MAR 2014

Assessment of the RegCM4 over East Asia and future precipitation change adapted to the RCP scenarios

Seok-Geun Oh[1], Ju-Hee Park[1], Sang-Hyun Lee[1], and Myoung-Seok Suh[1]

[1]Department of Atmospheric Science, Kongju National University, Gongju, South Korea

Abstract In this study, we investigated spatial and temporal changes in precipitation over the Coordinated Regional Climate Downscaling Experiment (CORDEX) East Asia domain, for present (1986–2005) and future (2031–2050) periods using the Regional Climate Model version 4 (RegCM4). Future meteorology produced by the Hadley Center Global Environmental Model version 2 coupled with the Atmosphere–Ocean (HadGEM2-AO) following global climate change scenarios (Representative Concentration Pathways (RCP) 4.5 and 8.5) was used as meteorological boundary conditions for the RegCM4. Six subregions (South Korea, North China, South China, Japan, Mongolia, and India) in the CORDEX East Asia domain were considered for analysis. The RegCM4 simulated spatial distributions of precipitation over East Asia with a correlation coefficient of 0.7 against Climate Research Unit data. The simulation skills of its temporal variability varied based on geographical regions and seasons, showing relatively poorer performance (underestimation in rainfall amount) in summer than in winter, in general. The future climate simulations by the RegCM4 presented that the East Asian continental regions will be warmer and more humid, leading to increased precipitation amounts, especially in the summer. The summer precipitation amount was projected to increase by about 5%, on average, over the East Asian domain, 5−15% in most subregions, and even higher (44% and 24%) in the South Korean region for the RCP 4.5 and 8.5 scenarios, respectively. It was also expected that heavy rainfall ($>$ 50 mm/d) events may occur more frequently in the future possibly owing to meteorological changes that are favorable to convective heavy precipitation.

1. Introduction

The background levels of atmospheric concentrations of anthropogenic greenhouse gases (e.g., CO_2, CH_4, and N_2O) have been continuously increasing since the industrial era, resulting in the currently observed climatic changes in the Earth's system (global warming). In particular, the enhancement in precipitable water due to the atmospheric temperature increase may change spatial and temporal variations of precipitation characteristics on regional and global scales [*Meehl et al.*, 2000; *Kimoto*, 2005; *Giorgi et al.*, 2011]. Several recent studies reported that the occurrence of abnormal weather phenomena (e.g., heavy rainfall, flood, and drought) is continuously increasing over East Asia [e.g., *Boo et al.*, 2006; *Gao et al.*, 2008; *Shi et al.*, 2009]. To cope with the adverse impacts associated with climate change on human beings, it might be of primary importance to understand and predict changes to the water cycle (or, specifically, precipitation).

For the fifth climate assessment report, planned to be published in 2013 by the Intergovernmental Panel on Climate Change, feasible future climate scenarios (that is, the Representative Concentration Pathways (RCP)) were developed in consideration of radiative forcing change by global warming culprits (e.g., greenhouse gases and aerosols) and recommended to use for future projection of possible global changes [*Moss et al.*, 2008].

The representative international intercomparison projects, the Coupled Models Intercomparison Project phase 5 and the Coordinated Regional Climate Downscaling Experiment (CORDEX), have been producing diverse climatological information on both global and regional scales with the guidance of the RCP scenarios [e.g., *Oh et al.*, 2011b; *Giorgi et al.*, 2012; *Taylor et al.*, 2012; *Suh et al.*, 2012; *Baek et al.*, 2013; *Lee et al.*, 2013; *Su et al.*, 2013; *Zou and Zhou*, 2013a]. Meanwhile, a dynamic downscaling approach using regional climate models (RCMs) has been popularly used in order to produce high-resolution regional climatology; this method was first adopted to overcome limitations in global climate models (GCMs) that has coarse spatial resolution (grid spacing ~100 km) and rather simple physical representation in the 1990s [e.g., *Giorgi*, 1990; *Giorgi et al.*, 1993; *Juang et al.*, 1997; *Lee and Suh*, 2000; *Suh and Lee*, 2004; *Kang et al.*, 2005].

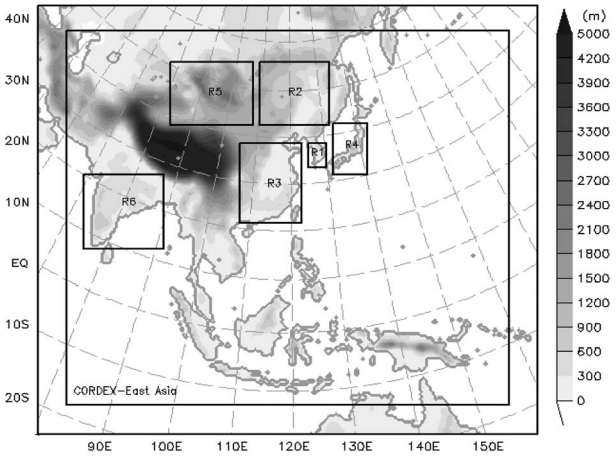

Figure 1. Model domain and analysis subregions. R1: South Korea (Latitude: 33°N–38°N, Longitude: 125°E–130°E), R2: North China (Latitude: 41°N–52°N, Longitude: 111°E–131°E), R3: South China (Latitude: 22°N–39°N, Longitude: 108°E–123°E), R4: Japan (Latitude: 30°N–42°N, Longitude: 131°E–141°E), R5: Mongolia (Latitude: 41°N–52°N, Longitude: 82°E–108°E), and R6: India (Latitude: 9°N–22°N, Longitude: 75°E–90°E). Topography (m) is shaded.

The performance of RCMs in simulating spatial and temporal variability at several atmospheric scales, as well as in simulating extreme meteorological events, has been evaluated in many studies through comparison of historical climate simulations against meteorological observations [e.g., *Kurihara et al*., 2005; *Boo et al*., 2006; *Shi et al*., 2009; *Oh et al*., 2013]. In previous studies, the RCMs reasonably reproduced atmospheric changes in temperature and wind fields but showed relatively poor performance in the simulation of precipitation at different geographical locations and during different seasons [e.g., *Dai et al*., 1999; *Giorgi and Shields*, 1999; *Feng and Fu*, 2006; *Im et al*., 2008; *Park et al*., 2008].

The understanding of the water cycle around the globe is essential to human life; thus, quantitative prediction of the behavior of the water cycle in a future climate with increased temperatures is of primary importance. Regional climate modeling is widely used as a promising tool for future projection of meteorological and hydrological conditions [e.g., *Gao et al*., 2008; *Giorgi et al*., 2011], but large uncertainties in future projection are associated with climate simulation models [e.g., *Giorgi et al*., 1993; *Giorgi and Shields*, 1999; *Im et al*., 2008; *Gao et al*., 2012; *Oh et al*., 2013]. Under the current situation, which does not allow any unique deterministic prediction for present and future climate simulations, a probabilistic interpretation that is based on multiple independent climate simulations may be necessary.

To contribute to this goal as part of the CORDEX project, we evaluate the performance of the Regional Climate Model version 4 (RegCM4) in simulating spatial and temporal characteristics of precipitation in different geographical regions over the CORDEX East Asia domain and then analyze climate modification of the precipitation patterns under different projected climate scenarios. Meteorological initial and boundary conditions for the RegCM4 have been obtained from the global climate simulation results of the Hadley Centre Global Environmental Model version 2 (HadGEM2-AO), which was run by the National Institute of Meteorological Research of the Korea Meteorological Administration (KMA) [*Baek et al*., 2013]. The model simulations were conducted for 72 years (1979–2050), and the simulations for the future period (2006–2050) were performed following the RCP 4.5 and 8.5 scenarios [*Moss et al*., 2008; *Baek et al*., 2013].

This manuscript is presented as follows. Section 2 describes the regional climate model and experimental setup for simulations of the present and future climatic conditions based on reliable global warming scenarios. Section 3 presents an evaluation of the model's performance in simulating precipitation patterns over the East Asian region. Section 4 discusses the change in precipitation patterns over the East Asia domain in a future climate and projects extreme precipitation conditions over the South Korean region. Discussion and conclusions follow in section 5.

2. Model and Experimental Setup

The RegCM4 used in this study is the latest version developed by the Abdus Salam International Centre for Theoretical Physics and has been widely applied to regional climate simulations [*Pal et al*., 2007]. The RegCM4 is a three-dimensional meteorological model, which adopts a hydrostatic assumption, the Arakawa B horizontal grid system, and a terrain-following sigma coordinate. It includes turbulence mixing, grid-scale and subgrid-scale cloud processes, radiative transfer processes, and land surface processes. Many physical processes of the model have been continuously updated since its previous version (http://www.ictp.it/research/esp/models/regcm4.aspx). More details on the model can be found in *Giorgi et al*. [2012].

Following the modeling framework of the CORDEX project, the simulation domain and horizontal grid spacing are set to the CORDEX East Asian domain and 50 km, respectively. Figure 1 shows the RegCM4 simulation

Table 1. Model Configuration Used in This Study

Contents	Description
Horizontal grid	243 × 197 (Δ*X* = 50 km)
Vertical layer (top)	18 sigma (50 hPa)
Turbulence	Holtslag scheme
Grid-scale cloud scheme	Subgrid explicit moisture scheme [*Pal et al*., 2000]
Cumulus parameterization	Emanuel scheme
Land surface processes	NCAR CLM3.5
Shortwave/longwave radiation	NCAR CCM3
Lateral boundary condition	HadGEM2-AO
Spectral nudging approach	*von Storch et al*. [2000]
Simulation period	Jan 1979 to Dec 2050 (72 years)

domain (12150 × 9850 km^2) that is centered on 22.04°N and 118.96°E with 243 × 197 grid mesh that covers most countries of Asia, southern Russia, the northern Indian Sea, and the western Pacific. Six subregions (South Korea, northern China, southern China, Japan, Mongolia, and India) are independently set as regional analysis zones to quantitatively investigate the model's performance and climatological change in precipitation over the regions. More intensive analyses are done in this study for the South Korean region, where precipitation data with a high spatial and temporal resolution are available from regular ground meteorological sites. The vertical grids are composed of 18 full sigma levels stretching from near the surface to the model top (50 hPa).

The parameterization of physical processes plays an important role in regional climate simulations. The cumulus parameterization scheme, in particular, is important for the simulation of precipitation [e.g., *Giorgi and Shields*, 1999]. In this study, the Emanuel cumulus parameterization scheme [*Emanuel*, 1991] is used for subgrid-scale cloud processes. The scheme showed better model performance in simulating precipitation in the South Korean region than other schemes from the 1 year sensitivity simulation [*Oh et al*., 2011a]. In combination with the cumulus parameterization, the subgrid explicit moisture scheme [*Pal et al*., 2000] is used for grid-scale cloud processes. The Holtslag turbulence scheme [*Holtslag et al*., 1990] is used in combination with the National Center for Atmospheric Research (NCAR) Community Land Model version 3.5 land surface model [*Oleson et al*., 2008; *Tawfik and Steiner*, 2011] and the NCAR Community Climate Model version 3 (CCM3) radiation scheme [*Kiehl et al*., 1996]. In addition, the spectral nudging technique was applied to the RegCM4 [*Park et al*., 2013] to reduce systematic errors that are commonly found in long-term simulations with a large simulation domain [*von Storch et al*., 2000; *Cha and Lee*, 2009]. The horizontal wind fields of the HadGEM2-AO with wavelengths over ~1000 km are nudged to the RegCM4 as a large-scale forcing. The model configuration is summarized in Table 1.

The model simulations were conducted between 1 January 1979 and 31 December 2050 with an integration time step of 100 s. The simulation outputs are saved every 3 h over the entire simulation period. The concentration of greenhouse gases and other agents are time varying during the simulation, which are taken from the RCP scenarios data group (http://www.pik-potsdam.de/~mmalte/rcps/). More description can be found in *Meinshausen et al*. [2011]. We then define two climatic time periods with a 20 year duration from the simulation period as present (1986–2005) and future (2031–2050) periods in order to examine the precipitation patterns during the different climatic periods.

The RegCM4-simulated precipitation for the present period is validated using multiple observational precipitation datasets of the Global Precipitation Climatology Project (GPCP) [*Adler et al*., 2003], the Climate Research Unit (CRU) time series 3.0 [*Mitchell and Jones*, 2005; *Harris et al*., 2013], and ground meteorological sites over South Korea. The GPCP data set used in this study is satellite-retrieved gridded monthly precipitation data covering the entire globe with a spatial resolution of 2°, thus allowing us to evaluate the model's ability to simulate temporal variations and spatial distributions of precipitation [*Adler et al*., 2003]. The CRU data set, based on surface observations, are gridded monthly precipitation data with a high spatial resolution (0.5° × 0.5°) but are only available for land areas [*Mitchell and Jones*, 2005; *Harris et al*., 2013]. The 59 ground meteorological sites operated by the KMA provide higher spatial (~12 km) and temporal (1 h) coverage of precipitation over the South Korean region than the others. The use of multiple data sets is beneficial not only to the evaluation of the model's simulation skills with high spatial and temporal scales but also to the verification of the observational datasets with one another. The analyses on both the model evaluation and precipitation characteristic patterns at different climatic periods and scenarios are mainly focused on the six subregions shown in Figure 1.

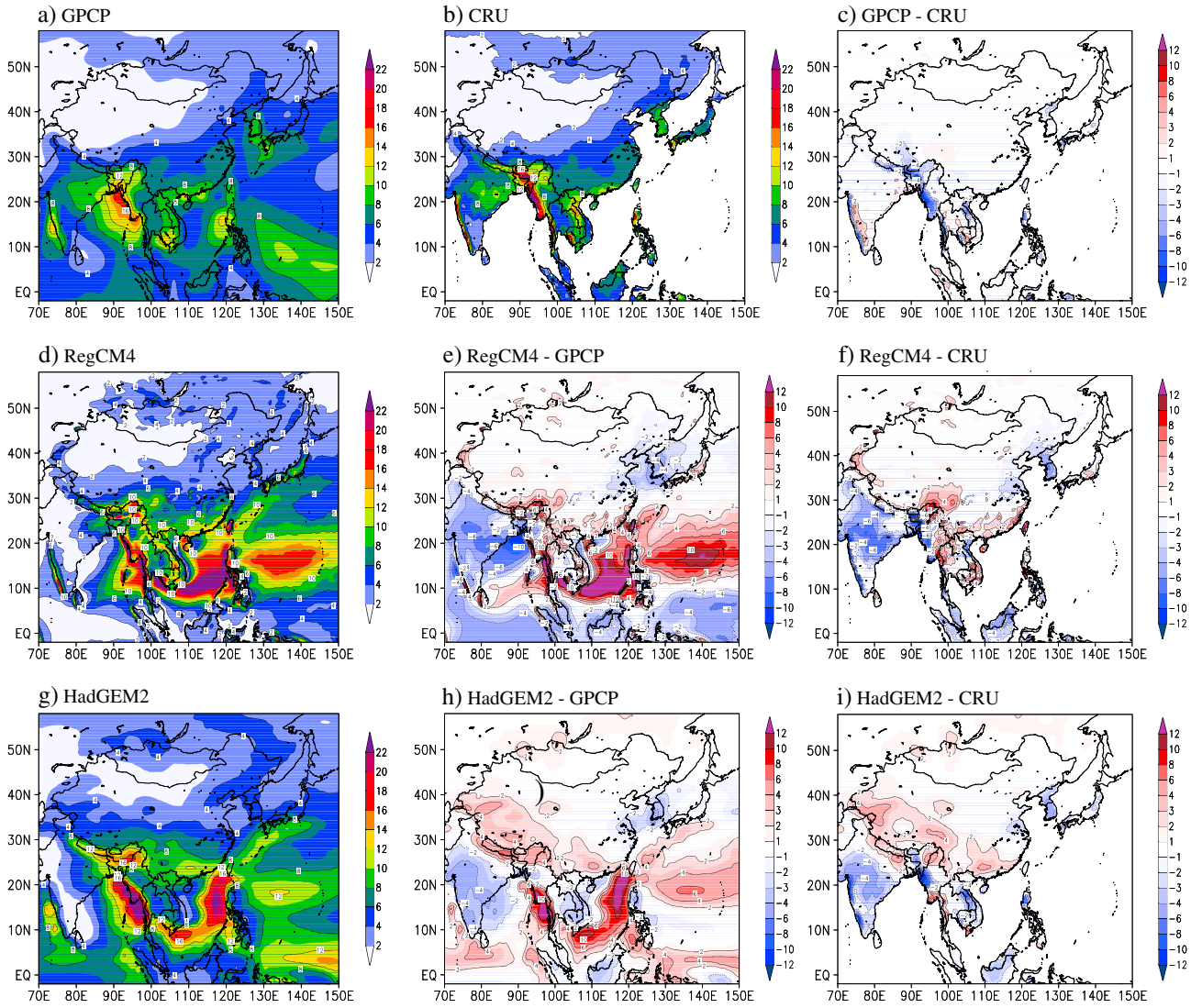

Figure 2. Spatial distributions of observed and simulated summer precipitations (mm/d) during summer (JJA) averaged for the present 20 year (1986–2005) period. (a) GPCP data, (b) CRU data, (c) difference between GPCP and CRU data, (d) RegCM4, (e) difference between RegCM4 and GPCP, (f) difference between RegCM4 and CRU, (g) HadGEM2, (h) difference between HadGEM2 and GPCP, and (i) difference between HadGEM2 and CRU.

3. Model Evaluation for the Present Climatic Period

3.1. Spatial Distribution of Seasonal Mean Precipitation

Figure 2 shows spatial distributions of the observed and simulated precipitation averaged for summer (June, July, and August (JJA)) during the present (1986–2005) period. The summer in the East Asian region can be characterized by heavy rains associated with summer monsoon compared to the other seasons. The summer monsoon rainbands are found both in the GPCP and CRU (Figures 2a and 2b), showing large amounts of precipitation in western India, northwestern area of the Indochinese peninsula, southern China, the Korean Peninsula, and southern Japan. The strongest rainband (10°N–25°N), with precipitation amounts over 16 mm/d, is also observed in the northeastern area of the Bay of Bengal (Figures 2a and 2b). The GPCP and CRU have similar spatial distributions over the region, but large differences over ±2 mm/d are found in highly elevated mountainous region and land/sea border region (e.g., Himalayan mountain range, western India, and Indochinese peninsula) (Figure 2c). Note that different spatial resolution between the two observations possibly induces the large differences. In addition, the CRU data can be oversmoothed in very complex terrain areas due to insufficient density of observation stations as discussed in the previous studies [e.g., *Bhaskaran et al.*, 1996; *Bergant et al.*, 2007];

thus, orographically induced precipitation in the model might be overestimated in comparison against the CRU in mountainous areas (Figure 2f).

The RegCM4 performs reasonably well in reproducing spatial distributions of the summer monsoon rainbands, but it overestimates precipitation by 5–20 mm/d mainly over ocean (the western Indochinese peninsula, the South China Sea, and the western Pacific); it underestimates precipitation by 2–10 mm/d in the Indian, South Korean, and the northern Bay of Bengal when compared to the GPCP and CRU data (Figures 2e and 2f). The HadGEM2-simulated precipitation has similar spatial distribution to that of the RegCM4 (Figure 2g) possibly due to spectral nudging of large-scale meteorology. The RegCM4 shows better agreement with the observations in Tibetan Plateau and southern China than the HadGEM2-AO, while its negative biases are larger in the India and South Korea regions. These simulation biases that depend on geographical location for precipitation were also reported from previous studies that used previous versions of the RegCM4 for the East Asian domain, in which the RCMs were driven by the global reanalysis data [e.g., *Suh and Lee*, 2004; *Park et al*., 2008] and GCM forecast [e.g., *Im et al*., 2008]. *Park et al*. [2013] performed sensitivity experiments with the RegCM4 using different global reanalysis data set (European Centre for Medium-Range Weather Forecasts Re-Analysis-Interim and National Centers for Environmental Prediction/NCAR reanalysis) to investigate the influence of lateral boundary conditions on precipitation over the CORDEX East Asia domain. Similar to the results of this study, the model overestimated summer precipitation for the South China Sea and the western Pacific but underestimated for India, South Korea, and the Bay of Bengal for both the different meteorological boundary conditions.

The model observation discrepancy might be attributed to several factors. In this study, the RegCM4 fails to simulate the exact location and development decay of the summer monsoon rainbands. In addition, an unrealistically simulated strong rainband, expanding in a subtropical maritime region (105°E−150°E; 10°N−20°N), may result in underestimated rainfall in the summer monsoon rainband [*Zou and Zhou*, 2011, 2013b].

Figure 3 shows spatial distributions of the observed and simulated precipitation averaged for winter (December, January, and February (DJF)) during the present (1986–2005) period. The rainbands in the winter period extend from southern parts of China to Japanese regions, and strong tropical rainbands near the equator are clear in the GPCP and CRU data (Figures 3a and 3b). The RegCM4 reasonably reproduces spatial distributions of the characteristic rainbands, but it overestimates precipitation by 2–4 mm/d in the winter rainbands and by over 6 mm/d in the tropical rainbands when compared to the GPCP data. Furthermore, the model overestimates the observations by 0–2 mm/d for inland regions of southern China and the Himalayan Mountain range. Like the summer season, the HadGEM2-simulated precipitation has a similar spatial distribution to that of the RegCM4 (Figure 3g).

Table 2 summarizes statistical evaluation results of the RegCM4 performance in the simulation of the spatial distribution of precipitation over the CORDEX East Asian domain and six subregions during the present (1986–2005) climate period. For the entire CORDEX East Asian domain, the model reasonably reproduces the spatial precipitation distribution with a spatial pattern correlation coefficient (R)/root-mean-square error (RMSE) of 0.62/3.89 mm/d in the summer and 0.74/2.21 mm/d in the winter, when compared with the CRU data. This result is comparable to that of *Lee et al*. [2013] that ran a regional climate model over the same domain and reported the values R/RMSE of 0.70/3.83 mm/d in the summer and 0.71/3.76 mm/d in the winter, compared to the same observation during a similar period (1980–2005). When compared to the GPCP data, which cover ocean area as well, the model's statistical performance degrades, indicating that the model's simulation skill over the region is higher for land than for ocean. This interpretation is supported by *Zou and Zhou* [2013b] that conducted precipitation simulations of summer monsoon over the western North Pacific domain (105°E−160°E; 0°N−40°N) using the RegCM3 with a model domain covering the Philippine Sea. Among sensitivity simulations, the best performance obtained showed the statistical values R/RMSE of 0.40/3.61 mm/d in a May–August period. It also shows that the model's summertime performance in simulating the spatial distribution of precipitation is generally inferior to that of the other seasons. In the analyses of the subregions, these statistical characteristics are consistently found, except in the Japanese and Mongolian regions, where the model shows relatively high performance. Relatively poor performance of the model is partially attributed to the use of coarse horizontal grid spacing ($\Delta X = 50$ km), which is not enough to fully resolve mesoscale convective systems that frequently occur in the summer over East Asia [*Ninomiya and Akiyama*, 1992; *Hong*, 2004; *Jhun and Lee*, 2004; *Park et al*., 2013].

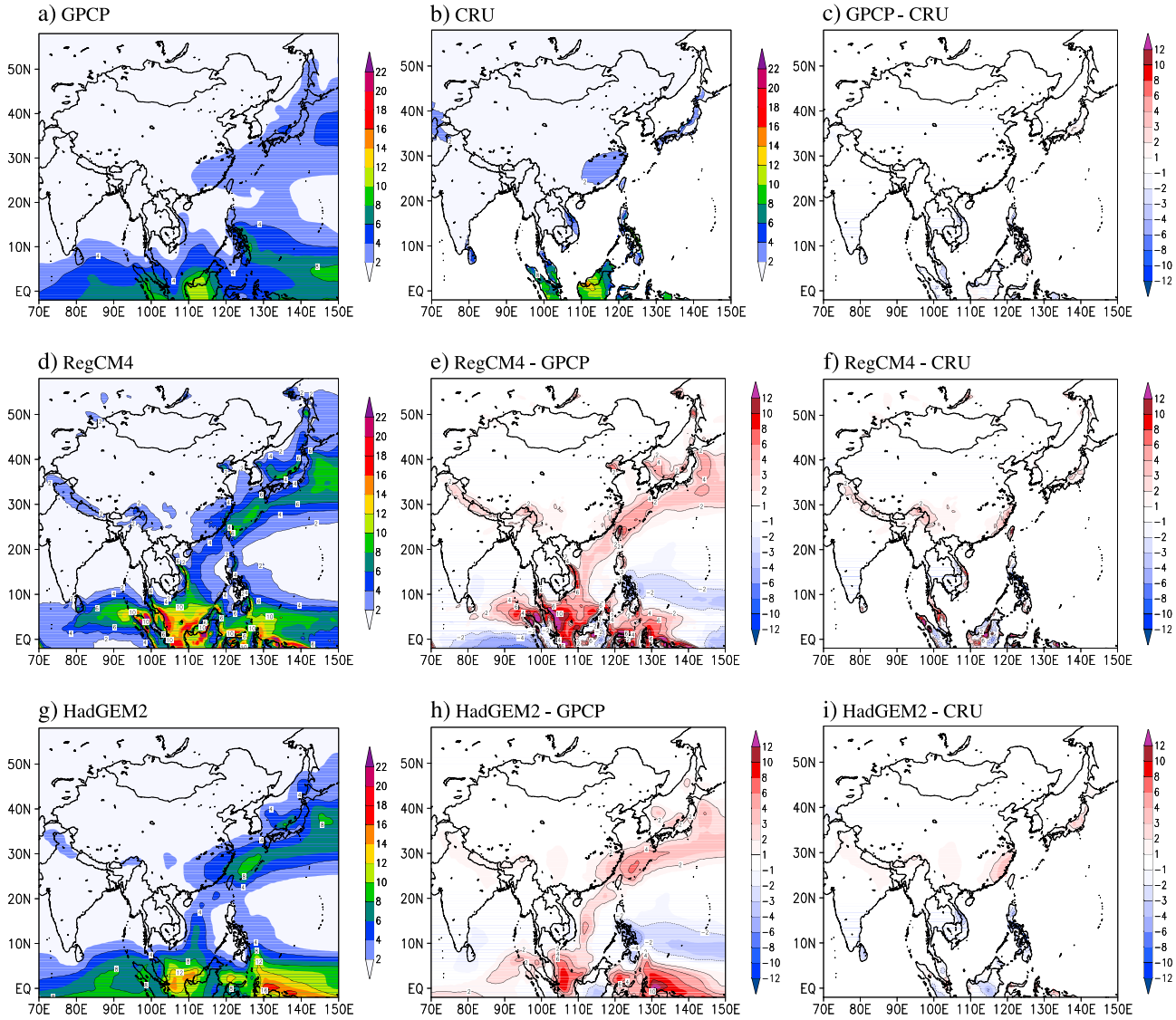

Figure 3. Same as Figure 2 except for winter (DJF).

3.2. Temporal Variation of Monthly Mean Precipitation

Figure 4 compares simulated monthly mean precipitation against the GPCP and CRU data for six subregions during the present period. Land grid cells both in the GPCP data and model simulation are averaged for the comparison, because the CRU data are only available over land. Similar to the spatial comparison between the GPCP and CRU data (Figures 2 and 3), the two observations have considerably similar temporal variations across all subregions; however, their precipitation amounts may differ by 0–1.5 mm/d at different locations and times. The spatial and temporal differences between the two observations can be interpreted as uncertainties in observed precipitation because the GPCP and CRU data are independently developed based mainly on satellite measurements and surface observations, respectively, at different spatial resolutions. When considering the magnitude of uncertainties in the observation, the RegCM4 reasonably reproduces seasonal variations of precipitation in most subregions ($R > 0.8$). The model's simulation skill is even higher in the regions of China and Mongolia with temporal correlation coefficients over 0.9. However, the model underestimates the observed precipitation amounts by 2–3 mm/d in the regions of South Korea, northern China, and India in the summer season. The simulated dry biases over the regions were reported similarly in the previous studies that have applied the RegCM3 [*Dash et al.*, 2006; *Gao et al.*, 2008; *Shi et al.*, 2009].

Table 2. Summary of Statistical Evaluation of the RegCM4 With the CRU Data for the Present 20 Year Period (1986–2005) Over the Entire East Asian Domain and Six Subregions[a]

Region	Evaluation	Annual	Spring	Summer	Autumn	Winter
CORDEX-EA	Mean	2.82	2.25	4.76	2.85	1.42
	(mm/d)	(3.75)	(3.26)	(5.34)	(3.98)	(2.40)
	Bias	0.00	0.32	−0.55	−0.21	0.45
	(mm/d)	(0.27)	(−0.18)	(0.26)	(0.11)	(0.87)
	RMSE	2.73	2.35	3.89	2.48	2.21
	(mm/d)	(3.83)	(3.02)	(5.28)	(3.41)	(3.62)
	R	0.70	0.72	0.62	0.72	0.74
		(0.53)	(0.57)	(0.47)	(0.58)	(0.52)
South Korea	Mean	4.07	3.00	9.06	2.95	1.26
	(mm/d)	(3.74)	(3.04)	(7.62)	(2.77)	(1.51)
	Bias	−1.52	−0.36	−5.24	−0.68	0.18
	(mm/d)	(−1.11)	(−0.31)	(−3.84)	(−0.37)	(0.09)
	RMSE	2.11	0.86	5.44	1.51	0.64
	(mm/d)	(1.93)	(1.07)	(4.27)	(1.69)	(0.71)
	R	0.48	0.56	0.26	0.57	0.53
		(0.37)	(0.66)	(0.21)	(0.15)	(0.46)
North China	Mean	1.60	0.94	4.23	1.07	0.16
	(mm/d)	(1.68)	(0.82)	(4.57)	(1.11)	(0.23)
	Bias	0.01	0.59	−1.18	0.26	0.36
	(mm/d)	(−0.07)	(0.71)	(−1.53)	(0.23)	(0.31)
	RMSE	0.83	0.69	1.65	0.55	0.43
	(mm/d)	(1.09)	(0.80)	(2.30)	(0.87)	(0.38)
	R	0.68	0.77	0.54	0.74	0.67
		(0.57)	(0.74)	(0.39)	(0.40)	(0.75)
South China	Mean	3.70	4.51	5.98	2.44	1.85
	(mm/d)	(3.30)	(3.94)	(5.34)	(2.75)	(1.18)
	Bias	0.35	0.17	0.28	0.26	0.68
	(mm/d)	(0.84)	(0.70)	(0.89)	(0.10)	(1.68)
	RMSE	2.23	2.05	3.63	1.56	1.69
	(mm/d)	(2.58)	(2.06)	(4.04)	(1.63)	(2.61)
	R	0.54	0.66	0.31	0.51	0.67
		(0.46)	(0.69)	(0.28)	(0.45)	(0.43)
Japan	Mean	5.03	4.44	7.61	5.58	2.51
	(mm/d)	(3.97)	(4.07)	(5.49)	(3.63)	(2.67)
	Bias	0.05	0.33	−0.91	−0.83	1.62
	(mm/d)	(0.91)	(0.43)	(−0.34)	(1.22)	(2.33)
	RMSE	2.60	1.71	3.14	2.92	2.60
	(mm/d)	(2.33)	(1.57)	(2.83)	(2.06)	(2.85)
	R	0.36	0.49	0.47	0.20	0.29
		(0.42)	(0.64)	(0.30)	(0.39)	(0.35)
Mongolia	Mean	0.72	0.37	1.97	0.46	0.08
	(mm/d)	(0.71)	(0.27)	(1.96)	(0.48)	(0.12)
	Bias	0.36	0.48	0.30	0.45	0.22
	(mm/d)	(0.38)	(0.58)	(0.31)	(0.44)	(0.18)
	RMSE	0.52	0.53	0.74	0.55	0.25
	(mm/d)	(0.57)	(0.63)	(0.88)	(0.56)	(0.23)
	R	0.65	0.64	0.79	0.64	0.52
		(0.52)	(0.56)	(0.76)	(0.31)	(0.44)
India	Mean	2.73	1.00	5.68	3.89	0.33
	(mm/d)	(3.25)	(1.05)	(6.73)	(4.33)	(0.91)
	Bias	−1.61	−0.56	−3.51	−2.59	0.22
	(mm/d)	(−1.66)	(−0.42)	(−4.11)	(−1.79)	(−0.31)
	RMSE	2.25	0.78	4.73	2.98	0.52
	(mm/d)	(2.20)	(0.74)	(4.81)	(2.56)	(0.67)
	R	0.54	0.45	0.49	0.66	0.56
		(0.40)	(0.21)	(0.42)	(0.54)	(0.44)

[a]Values in parenthesis indicate the evaluation results when the model is compared to the GPCP data. "Mean" indicates a mean value of CRU and GPCP data. "Bias" and *R* indicate that difference between simulation and observation and a spatial correlation, respectively.

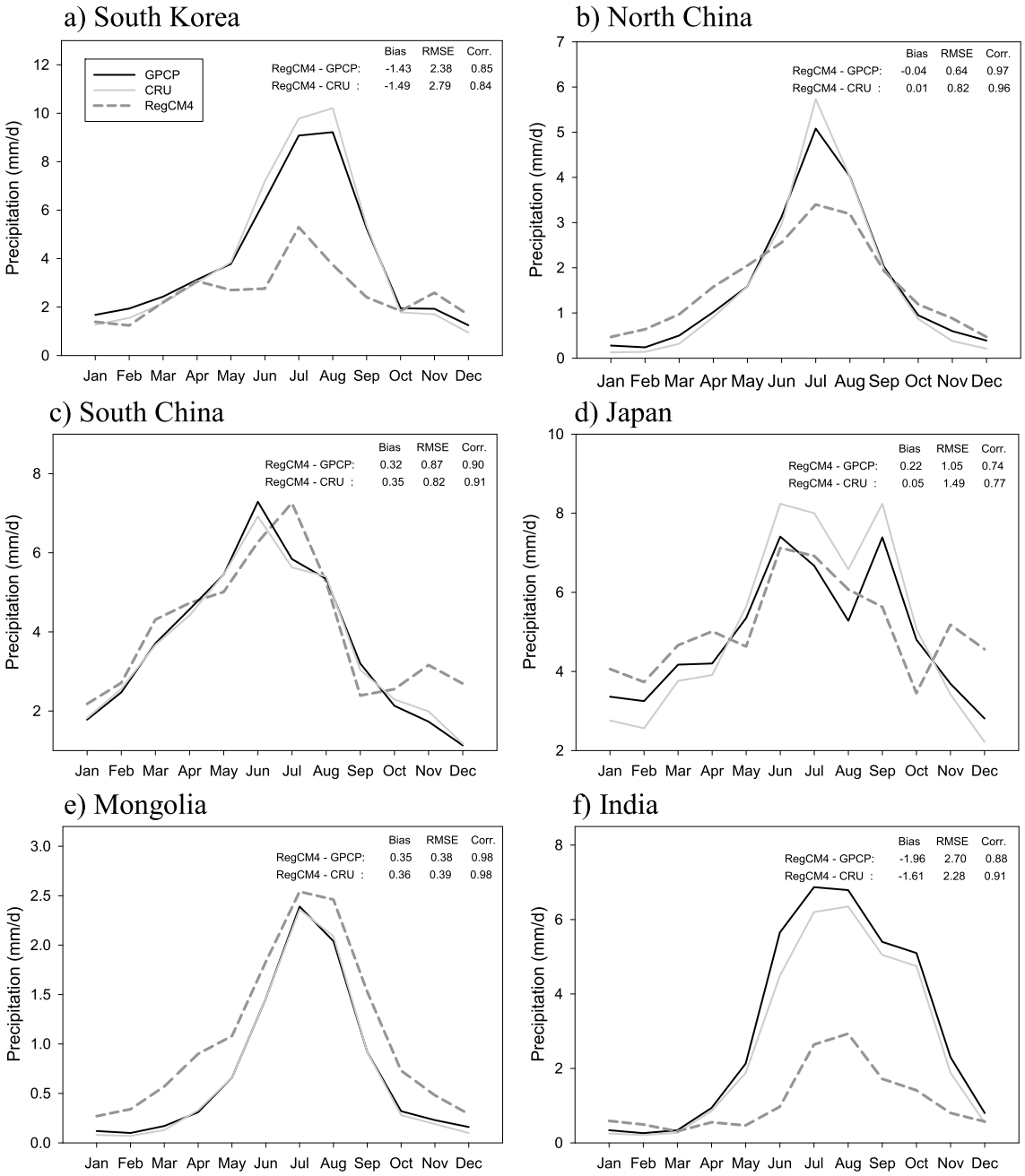

Figure 4. Monthly mean precipitation (mm/d) in GPCP and CRU data and in RegCM4 simulation for six subregions. The statistical characteristics were computed using regional monthly mean precipitation for each subregion.

Focusing on the South Korean region, the summertime precipitation is characterized by heavy rainfall associated with two meteorological conditions: a stationary front (locally named the *Changma* front) along the border of predominant air masses (the northwestern maritime Pacific High, the maritime Okhotsk High, and the continental Siberian High), which affects the region from mid-June to mid-July; and mesoscale convective systems (approximately tens of kilometers) under the predominant influence of the Pacific High until late August. During the JJA period, heavy rainfall events also occur sporadically by typhoons, which influence the Korean Peninsula more frequently after mid-July [*Park et al.*, 2006]. Figure 5 compares the simulated and observed daily mean precipitation averaged for the present 20 year period in the South Korean region for summer season (JJA). The subgrid-scale precipitation ratio (the ratio of the precipitation amounts calculated by cumulus parameterization to total precipitation) is overlaid to examine the relative contribution between

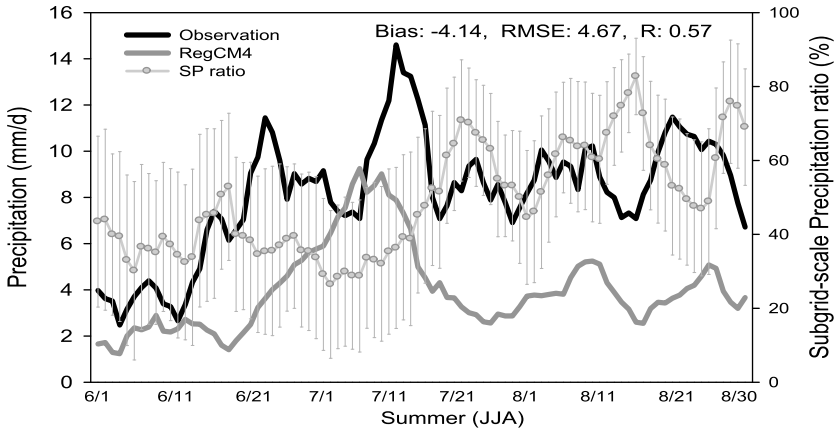

Figure 5. Time series of observed and simulated summer (JJA) daily mean precipitation (mm/d) in the South Korean region for the present 20 year (1986–2005) period. The SP ratio is defined by the ratio of subgrid-scale precipitation (SP) to the total precipitation in the simulation. Vertical bar indicates standard deviation. The observed precipitation is obtained as averaged values from 59 surface meteorological sites, operated by the KMA, and the simulation results are interpolated to the observation locations using a bilinear interpolation for comparison. A 5 day running mean is applied to both data. The statistical characteristics were computed using the daily mean precipitation.

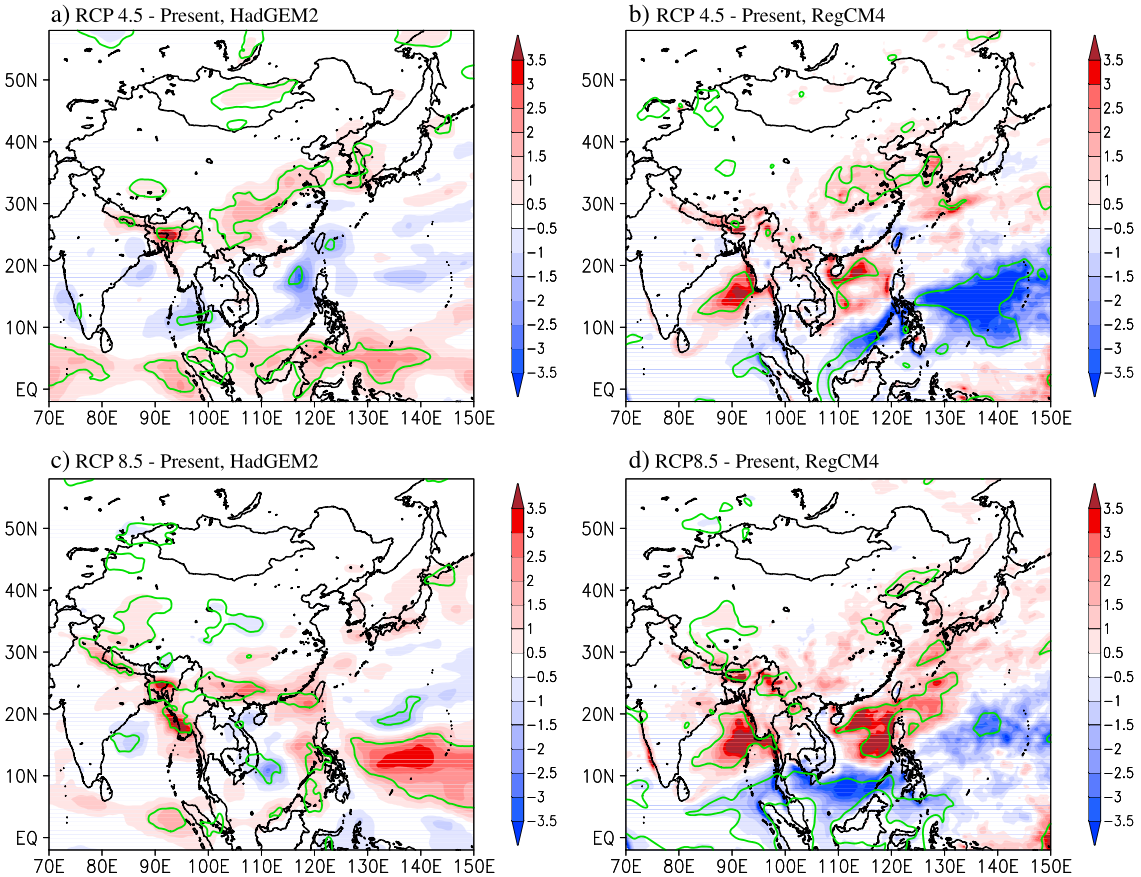

Figure 6. Spatial distributions of simulated seasonal mean precipitation change between future 20 year (2031–2050) and the present (1986–2005) periods in the summer (JJA): (a) HadGEM2-AO for RCP 4.5, (b) RegCM4 for RCP 4.5, (c) HadGEM2-AO for RCP 8.5, and (d) RegCM4 for RCP 8.5. The inside of closed contours (green line) indicates a statistically significant region at 5% significance level of *t* test.

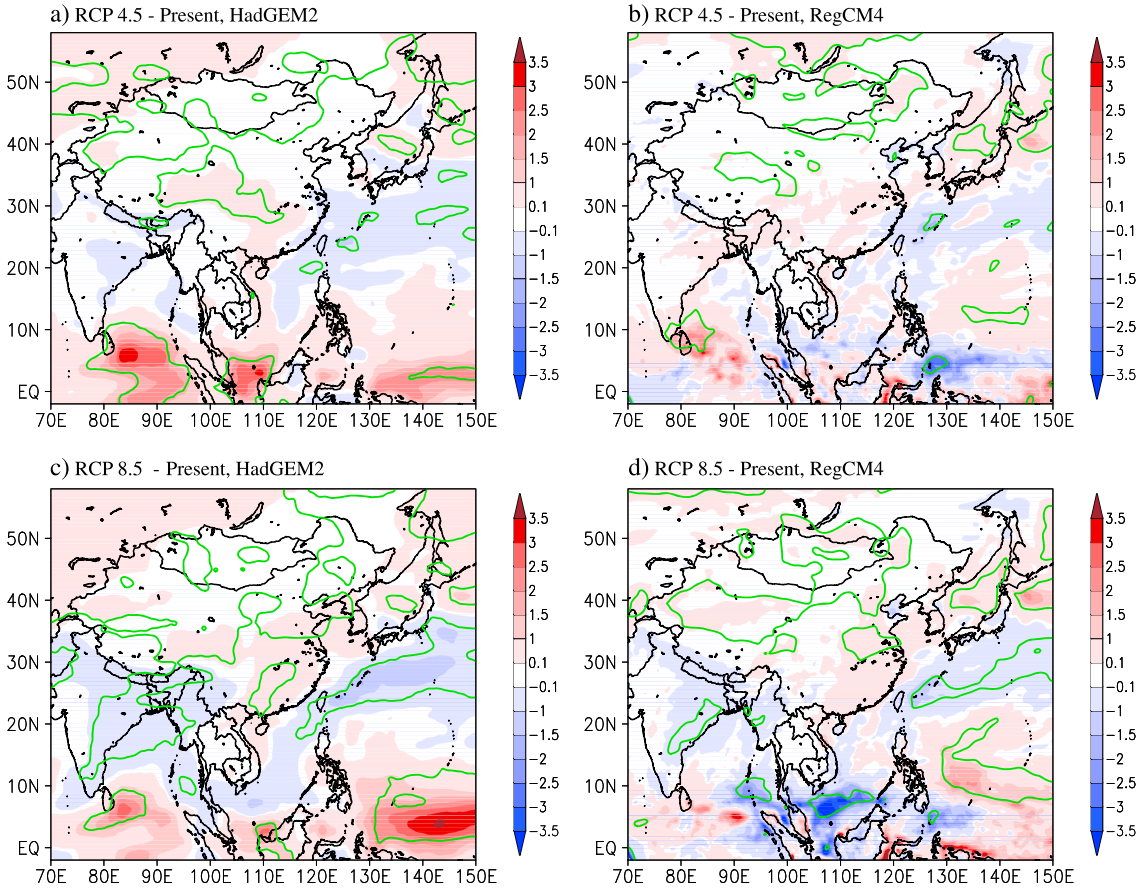

Figure 7. Same as Figure 6 except for winter (DJF). Note that the contour intervals are different from those in Figure 6.

grid-scale clouds and subgrid-scale cloud processes. The model regularly underestimates the observation throughout the summer period with a mean bias of −4.14 mm/d and a RMSE value of 4.67 mm/d, the result of which is consistent with Figure 4a. The model's negative bias (underestimation) is larger in late summer (−5.19 mm/d) than in early summer (−3.09 mm/d). *Park et al.* [2008] have reported the RegCM3 simulation results driven by the global reanalysis data, in which the model showed a similar temporal bias trend in simulating precipitation over South Korea in summer, showing that the negative biases in mid-July to August is greater than that in June to mid-July. A steep increase in the subgrid-scale precipitation ratio is found in mid-July as a cardinal point, which means that the model's atmospheric conditions are more favorable to convective initiation in the utilized cumulus parameterization. Interestingly, this corresponds roughly to the transition time of precipitation patterns from stationary frontal rains to mesoscale convective rains, suggesting that the reasonable cumulus parameterization should have a critical role for better simulation of precipitation in this region.

4. Future Precipitation Patterns

4.1. Spatial Distribution of Seasonal Mean Precipitation

The RegCM4 simulates that future meteorological conditions become warmer and more humid over the East Asian continental regions, which is more salient in the lower atmosphere than in the upper atmosphere especially in the summer (not shown). These meteorological changes are more favorable to precipitation due to enhancement of atmospheric thermal instability. Figures 6 and 7 present spatial distributions of seasonal mean precipitation differences between the present and future periods for the RCP 4.5 and 8.5 scenarios in terms of different seasons (summer and winter) and model simulations (HadGEM-AO and RegCM4), respectively. In each season, the simulated precipitation distributions for the different future climatic scenarios are spatially similar to those of the present precipitation patterns. Furthermore, the spatial distributions of the

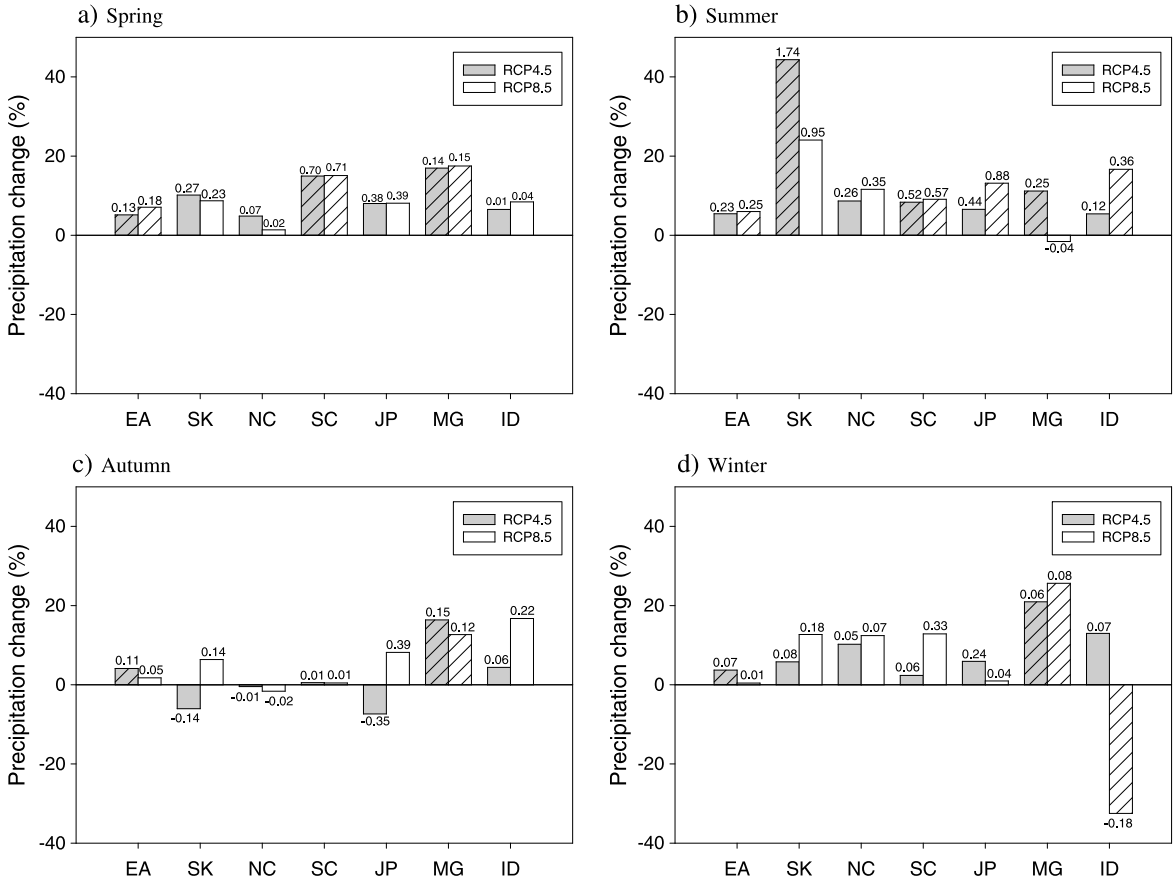

Figure 8. Fractional precipitation change [$(P_{future}-P_{present})/P_{present} \times 100$] between the present (1986–2005) and future (2031–2050) periods over the East Asian regions (EA: entire East Asia, SK: South Korea, NC: North China, SC: South China, JP: Japan, MG: Mongolia, and ID: India). Area mean changes of precipitation (mm/d) are given on the plot. The box filled with diagonal line indicates statistically significant change at 5% significance level of *t* test.

changes in the different seasons and climatic scenarios resemble those of the HadGEM2-AO global simulations, as might be expected [e.g., *Sung et al*., 2012; *Baek et al*., 2013]. The RegCM4 simulation shows that the summer monsoon rainbands expanding along Indian and Chinese-Korean-Japanese coastal regions will be intensified by up to 24 mm/d depending on the regions and climatic scenarios, while areas that are further inland, such as Mongolia, will experience little change due to small rainfall amounts during this season (Figure 6). The increasing trend of summer precipitation over the East Asian continental regions is also found in global climate [*Bao*, 2012; *Chen and Sun*, 2013; *Seo et al*., 2013] and the RCM simulations under RCP8.5 scenario [*Zou and Zhou*, 2013a]. Especially, the increase of precipitation under the RCP8.5 scenario is larger in the northern Bay of Bengal and the South China Sea than those of RCP4.5, whereas it is larger in Mongolia and South Korea in RCM4.5 than in RCP8.5. In the winter, the precipitation amounts are much smaller than those in the summer over the East Asian region (Table 2). In general, the increasing trend of future precipitation seen in the summer is also valid in the winter for most of the East Asian continental regions (Figure 7).

Figure 8 shows changes in fractional precipitation between the present and future climatic periods over the CORDEX East Asian domain and the six subregions in different seasons. The precipitation amounts for both the RCP scenarios are projected to be increased by approximately 5% in the spring and summer and less than that in the autumn and winter for the entire East Asian domain, while climatic changes in the six subregions are more apparent with larger fractional variations. Focusing on the summer season, which observes the most precipitation amounts of annual mean precipitations in all the region (Table 2), most salient precipitation enhancement is projected in the South Korean region with 44% and 24% increase for the RCP 4.5 and 8.5 scenarios, respectively, followed by the other regions with increases of 5–15%, when compared to the present precipitation. The relatively large difference in the South Korean region may be attributed partly to the small size of the analysis area as well (Figures 1 and 6). In the South China region, the model projects

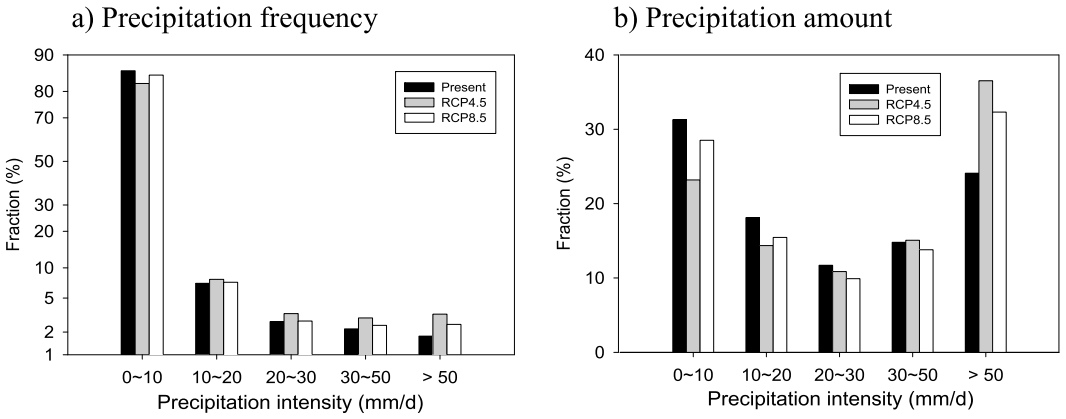

Figure 9. Fractional distributions of (a) precipitation frequency and (b) precipitation amount in terms of precipitation intensity over the South Korean region for summer (JJA). The model simulations for the present and the RCP 4.5 and 8.5 scenarios are compared. All bins except for a precipitation frequency bin of 20–30 mm/d in the RCP8.5 were statistically significant at 5% significance level of *Z* test.

about a 10% increase regardless of the RCP scenario used, but projects relatively large spatial variations ranging from negative values near southern coastal China to positive projections north of the area (Figure 6). The projection trends in the South Korean and Chinese regions are qualitatively consistent with the regional climate modeling results by *Lee et al*. [2013], which also used the same the global climate simulation results obtained from the HadGEM2-AO model. The projection trend of the South Korean region is also similar to the regional climate simulation results by *Gao et al*. [2012] that conducted dynamic downscaling with the RegCM3 over East Asia using different global climate simulations. However, the study reported that the future precipitation patterns in the Southern and Northern China regions are likely to have opposite signs, even when the global climate simulations used display the same increasing trend over the regions. More studies project the future precipitation over East Asia to increase in accordance with the global warming trend [e.g., *Kimoto*, 2005; *Kurihara et al*., 2005].

On the other hand, in the winter and other seasons in this study, the fractional increases of precipitation range from 5 to 20%, depending on the regions and the RCP scenarios used. The statistical significance of the changes tends to be lower than that in summer. Overall, more precipitation in future climate is projected over the regions for both the RCP4.5 and 8.5 scenarios, showing a small difference in precipitation amount between the scenarios.

4.2. Future Precipitation Patterns Over South Korea

The RegCM4 simulations indicate that the mean precipitation in summer over the South Korean region is increasing by +1.75 mm/d (44%) for the RCP 4.5 scenario and by +0.75 mm/d (24%) for the RCP 8.5 scenario. The change in this region is predominant when compared to the other subregions (Figure 8). In order to further investigate the future precipitation patterns over the South Korean region, we compare the precipitation amounts and occurrence frequency in terms of rain intensity in the summer between the present and future climatic periods (Figure 9). In the two different climatic scenarios, the model consistently projects that heavy rainfalls ($>$ 50 mm/d) increase in both the precipitation amount and occurrence frequency, whereas weak precipitation ($<$ 10 mm/d) events reduce over the South Korean region. Interestingly, the change in this study is relatively more prominent in the heavy rainfall bin. This result is similar to that of *Kimoto et al*. [2005] that analyzed the projected changes in precipitation around Japan using the coupled general circulation model.

Table 3. Number of Occurrence Day of Extreme Rainfall and the Number of Rainy Days in the Summer (JJA) Over South Korea[a]

	Present	RCP4.5	RCP8.5
Number of heavy rainfall ($>$ 80 mm/d)	0.40	1.03 (+157.5%)	0.71 (+77.5%)
Number of rainy days ($\geq$ 0.1 mm/d)	63.6	67.22 (+5.69%)	66.95 (+5.27%)

[a]The simulation results by the RegCM4 are analyzed for present (1986–2005) and future RCP 4.5 and 8.5 scenarios (2031–2050). The number in parenthesis indicates a fractional change of precipitation between the present and future period.

Table 3 summarizes the future projection of extreme precipitation events and the duration of the rainy period in summer over the South Korean region. The number of rainy days (≥ 0.1 mm/d) in the summer season (90 days) is about 64 days at the present climatic period and about 67 days for the RCP 4.5 and 8.5 scenarios; thus, a marginal increase in the number of precipitation day is expected. However, the number of intensive rainfall days (> 80 mm/d) has a statistically meaningful increase from 0.4 days per season at the present period to 1.03 days for the RCP 4.5 scenario and 0.71 days for the RCP 8.5 scenario, suggesting that extreme meteorological events such as intensive rainfalls and floods can be expected to increase in the future climate. This precipitation trend over the South Korean region has been consistently found in previous studies [e.g., *Boo et al*., 2006; *Im and Kwon*, 2007; *Sung et al*., 2012].

5. Discussion and Conclusions

The regional climate simulations were conducted using RegCM4 for 72 years (1979–2050) over the East Asian domain, focusing on climatic changes in precipitation in six subregions (South Korea, North China, South China, Japan, Mongolia, and India). The model domain and grid spacing (50 km) were configured following the recommendations of the CORDEX project to enable international intercomparison. The HadGEM2-AO simulations, representing different future climate scenarios, were used to drive dynamic downscaling over the region. In order to evaluate the RegCM4's performance in the simulation of spatial and temporal precipitation patterns, independent observational data sets of the GPCP and CRU data were used to validate the simulation results in the present climatic period. Surface meteorological monitoring data were also used to investigate high-resolution temporal characteristics of precipitation over the South Korean region.

The model reasonably reproduced the spatial distribution of precipitation over the East Asian domain with a spatial correlation of 0.62 in the summer and 0.74 in the winter, when compared to the CRU data. The monthly variation in precipitation, which can be characterized by the concentration of precipitation over East Asia in the summer, was well identified in both the GPCP and CRU data, with observation differences of 0–1 mm/d. The model also reproduced the characteristic temporal variations in all subregions but tended to underestimate the summer precipitation amount and overestimate the winter precipitation amount. This is partly attributed to the fact that the summer and winter precipitation over the East Asian region is predominantly produced by mesoscale convective systems and synoptic-scale frontal systems, respectively. The model's discrepancy was also identified by comparison with surface monitoring data over the South Korean region.

Based on the RegCM4 simulations, the future atmosphere represented by the RCP 4.5 and 8.5 scenarios were projected to be warmer and more humid over the East Asian continental regions than in the present, showing more prominent changes in the summer than in the other seasons. The precipitation amount in summer was increased by about 5% on average over the East Asian domain and ranged 5−15% (1–3 mm/d by amount) for the subregions, except for the South Korean region, where the most dramatic changes were expected (44% and 24% for the RCP 4.5 and 8.5 scenarios, respectively). It is likely that the increasing trend of precipitation over the China-Korea-Japan regions is associated with the enhanced low-level moisture advection and convective instability in the projected future atmosphere. Further analyses of future precipitation patterns over the South Korean region showed that heavy rainfall events (> 50 mm/d) may occur more frequently with enhanced intensities, whereas weak precipitation events were projected to have the opposite trend in rainfall amount and occurrence frequency. The increasing trends of precipitation amount and intensity were observed in the South Korean region [e.g., *Chung et al*., 2004; *Chang and Kwon*, 2007].

In this study, the analyses were performed with focus on the changes in precipitation over the East Asian continental regions. However, it was identified that the RegCM4 overestimated the GPCP data by 4–10 mm/d over the ocean of the South China Sea and the western Pacific Ocean (Figure 2, 10°N−20°N), resulting in degradation of the spatial correlation compared with the observation. Recently, similar biases were also reported by *Zou and Zhou* [2013b, 2013c], who attribute the discrepancy partly to the cumulus parameterization and local air-sea interaction. Therefore, it is perhaps reasonable to investigate the influence of the model's relatively poor performance over the oceanic region on the continental climatic patterns of precipitation for a reliable future projection.

Acknowledgments
This work was funded by the Korea Meteorological Administration Research and Development Program under grant CATER 2012–3081.

References

Adler, R. F., et al. (2003), The version-2 global precipitation climatology project (GPCP) monthly precipitation analysis (1979–present), *J. Hydrometeorol.*, *4*, 1147–1167.
Baek, H.-J., et al. (2013), Climate change in the 21st century simulated by HadGEM2-AO under representative concentration pathways, *APJAS*, *49*(5), 603–618, doi:10.1007/s13143-013-0053-7.
Bao, Q. (2012), Projected changes in Asian summer monsoon in RCP scenarios of CMIP5, *Atmos. Oceanic Sci. Lett.*, *5*(1), 43–48.
Bergant, K., M. Belda, and T. Halenka (2007), Systematic errors in the simulation of European climate (1961–2000) with RegCM3 driven by NCEP/NCAR reanalysis, *Int. J. Clim.*, *27*(4), 455–472.
Bhaskaran, B., R. G. Jones, J. M. Murphy, and M. Noguer (1996), Simulations of the Indian summer monsoon using a nested regional climate model: Domain size experiments, *Clim. Dyn.*, *12*, 573–587.
Boo, K.-O., W.-T. Kwon, and H.-J. Beak (2006), Change of extreme events of temperature and precipitation over Korea using regional projection of future climate change, *Geophys. Res. Lett.*, *33*, L01701, doi:10.1029/2005GL023378.
Cha, D.-H., and D.-K. Lee (2009), Reduction of systematic errors in regional climate simulations of the summer monsoon over East Asia and the western North Pacific by applying the spectral nudging technique, *J. Geophys. Res.*, *114*, D14108, doi:10.1029/2008JD011176.
Chang, H.-J., and W.-T. Kwon (2007), Spatial variations of summer precipitation trends in South Korea, 1973–2005, *Environ. Res. Lett.*, *2*, 1–9, doi:10.1088/1748-9326/2/4/04512.
Chen, H., and J. Sun (2013), Projected change in East Asian summer monsoon precipitation under RCP scenario, *Meteorol. Atmos. Phys.*, *121*, 55–77.
Chung, Y.-S., M.-B. Yoon, and H.-S. Kim (2004), On climate variations and changes observed in South Korea, *Clim. Change*, *66*, 151–161.
Dai, A., F. Giorgi, and K. E. Trenberth (1999), Observed and model-simulated diurnal cycles of precipitation over the contiguous United States, *J. Geophys. Res.*, *104*, 6377–6402, doi:10.1029/98JD02720.
Dash, S. K., M. S. Shekhar, and G. P. Singh (2006), Simulation of Indian summer monsoon circulation and rainfall using RegCM3, *Theor. Appl. Climatol.*, *86*, 161–172.
Emanuel, K. A. (1991), A scheme for representing cumulus convection in large-scale models, *J. Atmos. Sci.*, *48*, 2313–2329.
Feng, J., and C. Fu (2006), Inter-comparison of 10-year precipitation simulated by several RCMs for Asia, *Adv. Atmos. Sci.*, *23*, 531–542.
Gao, X., Y. Shi, R. Song, F. Giorgi, Y. Wang, and D. Zhang (2008), Reduction of future monsoon precipitation over China: Comparison between a high resolution RCM simulation and the driving GCM, *Meteorol. Atmos. Phys.*, *100*, 73–86, doi:10.1007/s00703-008-0296-5.
Gao, X., Y. Shi, D. Zhang, J. Wu, F. Giorgi, Z. Ji, and Y. Wang (2012), Uncertainties in monsoon precipitation projections over China: Results from two high-resolution RCM simulations, *Clim. Res.*, *52*(2), 213–226.
Giorgi, F. (1990), Simulation of regional climate using a limited area model nested in a general circulation model, *J. Clim.*, *3*, 941–963.
Giorgi, F., and C. Shields (1999), Tests of precipitation parameterization available in the latest version of the NCAR regional climate model (RegCM) over the continental United States, *J. Geophys. Res.*, *104*, 6353–6375.
Giorgi, F., M. R. Marinucci, and G. T. Bates (1993), Development of a second-generation regional climate model (RegCM2), Part I: Boundary-layer and radiative processes, *Mon. Weather Rev.*, *121*, 2794–2813.
Giorgi, F., E. S. Im, E. Coppola, N. S. Diffenbaugh, X. J. Gao, L. Matiotti, and Y. Shi (2011), Higher hydroclimatic intensity with global warming, *J. Clim.*, *24*, 5309–5324.
Giorgi, F., et al. (2012), RegCM4: Model description and preliminary test over multiple CORDEX domains, *Clim. Res.*, *52*, 7–29.
Harris, I., P. D. Jones, T. J. Osborn, and D. H. Lister (2013), Updated high-resolution grids of monthly climatic observations—The CRU TS3.10 dataset, *Int. J. Climatol.*, doi:10.1002/joc.3711, in press.
Holtslag, A. A. M., E. I. F. De Bruijn, and H. L. Pan (1990), A high resolution air mass transformation model for short-range weather forecasting, *Mon. Weather Rev.*, *118*, 1561–1575.
Hong, S.-Y. (2004), Comparison of heavy rainfall mechanisms in Korea and the Central US, *J. Meteorol. Soc. Jpn.*, *82*(5), 1469–1479.
Im, E.-S., and W.-T. Kwon (2007), Characteristics of extreme climate sequences over Korea using regional climate change scenario, *SOLA*, *3*, 17–20, doi:10.2151/sola.2007-005.
Im, E.-S., J.-B. Ahn, A. R. Remedio, and W.-T. Kwon (2008), Sensitivity of the regional climate of East/Southeast Asia to convective parameterizations in the RegCM3 modeling system. Part 1: Focus on the Korean peninsula, *Int. J. Climatol.*, *28*, 1861–1877.
Jhun, J.-G., and E.-J. Lee (2004), A new East Asian winter monsoon index and associated characteristics of the winter monsoon, *J. Clim.*, *17*(4), 711–726.
Juang, H. M. H., S.-Y. Hong, and M. Kanamitsu (1997), The NCEP regional spectral model: An update, *Bull. Am. Meteorol. Soc.*, *78*, 2125–2143.
Kang, H.-S., D.-H. Cha, and D.-K. Lee (2005), Evaluation of the mesoscale model/land surface model(MM5/LSM) coupled model for East Asian summer monsoon simulations, *J. Geophys. Res.*, *110*, D10105, doi:10.1029/2004JD005266.
Kiehl, J. T., J. J. Hack, G. B. Bonan, B. A. Boville, B. P. Briegleb, D. L. Williamson, and P. J. Rasch (1996), Description of NCAR Community Climate Model (CCM3), *NCAR Tech. Note NCAR/TN-420+STR*, 152 pp.
Kimoto, M. (2005), Simulated change of the East Asian circulation under the global warming scenario, *Geophys. Res. Lett.*, *32*, L16701, doi:10.1029/2005GL023383.
Kimoto, M., N. Yasutomi, C. Yokoyama, and S. Emori (2005), Projected changes in precipitation characteristics around Japan under the Global Warming, *SOLA*, *1*, 085–088.
Kurihara, K., K. Ishihara, H. Sasaki, Y. Fukuyama, H. Saitou, I. Takayabu, K. Murazaki, Y. Sato, S. Yukimoto, and A. Noda (2005), Projection of climate change over Japan due to global warming by high resolution regional climate model in MRI, *SOLA*, *1*, 97–100, doi:10.2151/sola.
Lee, D.-K., and M.-S. Suh (2000), Ten-year East Asian summer monsoon simulation using a regional climate model (RegCM2), *J. Geophys. Res.*, *105*, 29,565–29,577.
Lee, J.-W., S.-Y. Hong, E.-C. Chang, M.-S. Suh, and H.-S. Kang (2013), Assessment of future climate change over East Asia due to the RCP scenarios downscaled by GRIMs-RMP, *Clim. Dyn.*, *42*, 733–747, doi:10.1007/s00382-013-1841-6.
Meehl, G. A., F. Zwiers, J. Evans, T. Knutson, L. Mearns, and P. Whetton (2000), Trends in extreme weather and climate events: Issues related to modeling extremes in projections of future climate change, *Bull. Am. Meteorol. Soc.*, *81*(3), 427–436.
Meinshausen, M., et al. (2011), The RCP greenhouse gas concentrations and their extensions from 1765 to 2300, *Clim. Change*, *109*, 213–241.
Mitchell, T. D., and P. D. Jones (2005), An improved method of constructing a database of monthly climate observations and associated high-resolution grids, *Int. J. Climatol.*, *25*(6), 693–712.
Moss, R., et al. (2008), Towards new scenarios for analysis of emissions, climate change, impacts, and response strategies, Technical Summary, *Intergovernmental Panel on Climate Change, Geneva*, 25 pp.
Ninomiya, K., and T. Akiyama (1992), Multi-scale features of Baiu, the summer monsoon over Japan and the East Asia, *J. Meteorol. Soc. Jpn.*, *70*, 467–495.

Oh, S.-G., M.-S. Suh, J.-S. Myoung, and D.-H. Cha (2011a), Impact of boundary conditions and cumulus parameterization schemes on regional climate simulation over South-Korea in the CORDEX-East Asia domain using the RegCM4 model [in Korean with English abstract], *J. Korean Earth Sci. Soc.*, *32*, 373–387.

Oh, S.-G., M.-S. Suh, D.-H. Cha, and S.-J. Choi (2011b), Simulation skills of RegCM4 for regional climate over CORDEX East Asia driven by HadGEM2-AO [in Korean with English abstract], *J. Korean Earth Sci. Soc.*, *32*, 732–749.

Oh, S.-G., M.-S. Suh, and D.-H. Cha (2013), Impact of lateral boundary conditions on precipitation and temperature extremes over South Korea in the CORDEX regional climate simulation using RegCM4, *APJAS*, *49*(4), 497–509, doi:10.1007/s13143-013-0044-8.

Oleson, K. W., et al. (2008), Improvements to the community land model and their impact on the hydrological cycle, *J. Geophys. Res.*, *113*, G01021, doi:10.1029/2007JG000563.

Pal, J. S., E. Small, and E. Eltahir (2000), Simulation of regional-scale water and energy budgets: Representation of subgrid cloud and precipitation processes within RegCM, *J. Geophys. Res.*, *105*, 29,579–29,594.

Pal, J. S., et al. (2007), Regional climate modeling for the developing world: The ICTP RegCM3 and RegCNET, *Bull. Am. Meteorol. Soc.*, *88*, 1395–1409.

Park, E.-H., S.-Y. Hong, and H.-S. Kang (2008), Characteristics of an East-Asian summer monsoon climatology simulated by the RegCM3, *Meteorol. Atmos. Phys.*, *100*, 139–158.

Park, J.-H., S.-G. Oh, and M.-S. Suh (2013), Impacts of boundary conditions on the precipitation simulation of RegCM4 in the CORDEX East Asia domain, *J. Geophys. Res. Atmos.*, *118*, 1652–1667, doi:10.1002/jgrd.50159.

Park, J.-K., B.-S. Kim, W.-S. Jung, E.-B. Kim, and D.-G. Lee (2006), Change in statistical characteristics of typhoon affecting the Korean Peninsula [in Korean with English abstract], *Atmosphere*, *16*(1), 1–17.

Seo, K.-H., J. Ok, J.-H. Son, and D.-H. Cha (2013), Assessing future changes in the East Asian summer monsoon using CMIP5 coupled models, *J. Clim.*, *26*, 7662–7675.

Shi, Y., X. J. Gao, Y. G. Wang, and F. Giorgi (2009), Simulation and projection of monsoon on rainfall and rain patterns over eastern China under global warming by RegCM3, *Atmos. Oceanic Sci. Lett.*, *2*(5), 308–313.

Su, F., X. Duan, D. Chen, Z. Hao, and L. Cuo (2013), Evaluation of the global climate models in the CMIP5 over the Tibetan Plateau, *J. Clim.*, *26*, 3187–3208.

Suh, M.-S., and D.-K. Lee (2004), Impacts of land use/cover changes on surface climate over east Asia for extreme climate cases using RegCM2, *J. Geophys. Res.*, *109*, D02108, doi:10.1029/2003JD003681.

Suh, M.-S., S.-G. Oh, D.-K. Lee, D.-H. Cha, S.-J. Choi, C.-S. Jin, and S.-Y. Hong (2012), Development of new ensemble methods based on the performance skills of regional climate models over South Korea, *J. Clim.*, *25*, 7067–7082.

Sung, J.-H., H.-S. Kang, S.-H. Park, C.-H. Cho, D.-H. Bae, and Y.-O. Kim (2012), Projection of extreme precipitation at the end of 21st century over South Korea based on representative concentration pathways (RCP) [in Korean with English abstract], *Atmosphere*, *22*(2), 221–231.

Tawfik, A. B., and A. L. Steiner (2011), The role of soil ice in land-atmosphere coupling over the United States: A soil moisture precipitation winter feedback mechanism, *J. Geophys. Res.*, *116*, D02113, doi:10.1029/2010JD014333.

Taylor, K. E., R. J. Stouffer, and G. A. Meehl (2012), An overview of CMIP5 and the experiment design, *Bull. Am. Meteorol. Soc.*, *93*(4), 485–498.

von Storch, H., H. Langerberg, and F. Feser (2000), A spectral nudging technique for dynamical downscaling purposes, *Mon. Weather Rev.*, *128*, 3664–3673.

Zou, L., and T. Zhou (2011), Sensitivity of a regional ocean–atmosphere coupled model to convection parameterization over western North Pacific, *J. Geophys. Res.*, *116*, D18106, doi:10.1029/2011JD015844.

Zou, L., and T. Zhou (2013a), Near future (2016–40) summer precipitation changes over China as projected by a regional climate model (RCM) under the RCP8.5 emissions scenario: Comparison between RCM downscaling and the driving GCM, *Adv. Atmos. Sci.*, *30*(3), 806–818, doi:10.1007/s00376-013-2209-x.

Zou, L., and T. Zhou (2013b), Improve the simulation of western North Pacific summer monsoon in RegCM3 by suppressing convection, *Meteorol. Atmos. Phys.*, *121*, 29–38.

Zou, L., and T. Zhou (2013c), Can a regional ocean–atmosphere coupled model improve the simulation of the interannual variability of the western North Pacific summer monsoon?, *J. Clim.*, *26*(7), 2353–2367.